Research Article

Journal of Molecular Recognition

Received: 1 December 2009, Revised: 17 March 2010, Accepted: 18 March 2010, Published online in Wiley InterScience: 2010

(www.interscience.wiley.com) DOI:10.1002/jmr.1042

The interaction of Jagged-1 cytoplasmic tail with afadin PDZ domain is local, folding-independent, and tuned by phosphorylation

Matija Popovic[a], Juraj Bella[b], Ventsislav Zlatev[a], Vesna Hodnik[c], Gregor Anderluh[c], Paul N. Barlow[b], Alessandro Pintar[a]* and Sándor Pongor[a]*

Jagged-1, one of the five Notch ligands in man, is a membrane-spanning protein made of a large extracellular region and a 125-residue cytoplasmic tail bearing a C-terminal PDZ recognition motif (^{1213}RMEYIV^{1218}). Binding of Jagged-1 intracellular region to the PDZ domain of afadin, a protein located at cell–cell adherens junctions, couples Notch signaling with the adhesion system and the cytoskeleton. Using NMR chemical shift perturbation and surface plasmon resonance, we studied the interaction between the PDZ domain of afadin (AF6_PDZ) and a series of polypeptides comprising the PDZ-binding motif. Chemical shift mapping of AF6_PDZ upon binding of ligands of different length (6, 24, and 133 residues) showed that the interaction is strictly local and involves only the binding groove in the PDZ. The recombinant protein corresponding to the entire intracellular region of Jagged-1, J1_ic, is mainly disordered in solution, and chemical shift mapping of J1_ic in the presence of AF6_PDZ showed that binding is not coupled to folding. Binding studies on a series of 24-residue peptides phosphorylated at different positions showed that phosphorylation of the tyrosine at position -2 of the PDZ-binding motif decreases its affinity for AF6_PDZ, and may play a role in the modulation of this interaction. Finally, we show that the R1213Q mutation located in the PDZ-binding motif and associated with extrahepatic biliary atresia increases the affinity for AF6_PDZ, suggesting that this syndrome may arise from an imbalance in the coupling of Notch signaling to the cytoskeleton.

Supporting information may be found in the online version of this paper.

Keywords: Notch signaling; intrinsic disorder; disease mutation; NMR; chemical shift mapping; surface plasmon resonance

INTRODUCTION

Signaling mediated by Notch receptors and their ligands is essential both in the developing embryo, where it drives lineage decisions and organogenesis, and in adult cells, where it controls cell fate in a strongly context-dependent manner (Gordon *et al*., 2008; Kopan and Ilagan, 2009). Notch ligands (Jagged-1 and -2, Delta-like-1, -3, and -4 in man) are membrane-spanning proteins with a large extracellular region and a 100–150 residue cytoplasmic tail. Intracellular regions, while lacking globular domains, are highly conserved within the same ligand type, consistent with possession of specific biological functions (Pintar *et al*., 2007). In addition to ubiquitination-mediated ligand endocytosis (Brou, 2009) and regulated intra-membrane proteolysis, the cytoplasmic tails of Notch ligands (Hock *et al*., 1998; Ascano *et al*., 2003; Carmena *et al*., 2006) couple the Notch signaling pathway to PDZ-containing, membrane-associated proteins that play a role in the organization of cell–cell junctions (Zhang and Wang, 2003). PDZ domains (Kay and Kehoe, 2004), which are among the most recurrent intracellular protein interaction modules, are made of six β-strands and two α-helices that fold in the β-roll topology (CATH: 2.30.42). Most commonly, PDZ domains bind the C-terminal segment of the target protein in a groove between the second β-strand (βB) and the second α-helix (αB) of the PDZ domain, with the free carboxyl terminus of the target protein involved in a key interaction with the βA/βB loop of the PDZ. The ligand is bound in an extended conformation, as an antiparallel β-strand complementing the

* *Correspondence to: A. Pintar or S. Pongor, Protein Structure and Bioinformatics Group, International Centre for Genetic Engineering and Biotechnology (ICGEB), AREA Science Park, Padriciano 99, I-34149 Trieste, Italy. E-mail: pintar@icgeb.org; pongor@icgeb.org*

a *M. Popovic, V. Zlatev, A. Pintar, S. Pongor, A. Pintar, S. Pongor Protein Structure and Bioinformatics Group, International Centre for Genetic Engineering and Biotechnology (ICGEB), AREA Science Park, Padriciano 99, I-34149 Trieste, Italy*

b *J. Bella, P. N. Barlow Biomolecular NMR Unit, Schools of Biological Sciences and Chemistry, University of Edinburgh, West Mains Road, Edinburgh EH9 3JJ, UK*

c *V. Hodnik, G. Anderluh Department of Biology, Biotechnical Faculty, University of Ljubljana, Večna pot 111, 1000 Ljubljana, Slovenia*

βB strand, with very little perturbation of the structure of the PDZ domain (Remaut and Waksman, 2006). Binding specificity was initially assigned according to the nature of the last four amino acid residues of the PDZ binding motif (identified as P-0, P-1, P-2, P-3, where P-0 is the C-terminus), and divided into class I (x-Ser/Thr-x-Φ-COOH, where x can be any amino acid residue, and Φ is a hydrophobic residue) and class II (x-Φ-x-Φ-COOH) (Songyang *et al*., 1997). More recent studies, however, suggest that specificity is achieved through a subtle interplay between the sequence of the PDZ-binding motif and the sequence of the PDZ itself (Chen *et al*., 2008; Tonikian *et al*., 2008; Wiedemann *et al*., 2004), with K_d values that can vary widely between 1 and 100 μM (Stiffler *et al*., 2007). A PDZ-binding motif is located at the C-terminus of the cytoplasmic tail of Jagged-1 (RMEYIV-COOH, class II) and of Delta-1/4, (ATEV-COOH, class I) but not in Jagged-2 and Delta-3. In yeast two-hybrid assays, the C-terminal hexapeptide from Jagged-1 was shown to bind the PDZ domain of actin filament-binding protein (afadin, also known as AF-6 or MLLT4), one of the components in cell–cell adherens junctions (Hock *et al*., 1998). The interaction between the cytoplasmic tail of Jagged-1 and afadin was confirmed by GST-pulldown experiments on whole cell lysates from transiently transfected 293T cells expressing myc-tagged afadin (Ascano *et al*., 2003). Deletion of either the PDZ-binding motif from the GST-Jagged-1 fusion protein or of the PDZ from afadin abolished the interaction (Ascano *et al*., 2003).

In the present work, we examine, for the first time, the mode of binding of Jagged-1 cytoplasmic tail to the afadin PDZ domain and question whether binding to the PDZ domain may induce folding in the structurally disordered Jagged-1 cytoplasmic tail. We investigate whether phosphorylation at key residues in or near the PDZ-binding motif may modulate this interaction and we report the first chemical shift mapping study with phosphorylated peptides as ligands. We also address, for the first time, the molecular grounds of a morphological disorder, extrahepatic biliary atresia, associated with a sporadic R1213Q mutation in Jagged-1 cytoplasmic tail.

MATERIALS AND METHODS

Protein expression and purification

The unlabeled and ^{15}N-labeled recombinant proteins corresponding to Jagged-1 intracellular region (J1_ic, residues 1086–1218 of JAG1_HUMAN) were expressed in BL21(DE3) *E. coli* (Novagen) cells from a codon-optimized synthetic gene cloned into a pET-11a vector (Novagen), purified in two steps by IMAC (Ni^{2+}-Sepharose HisTrap HP column) and RP-HPLC, as described (Popovic *et al*., 2007), and freeze-dried.

The afadin PDZ domain (AF6_PDZ, residues 987–1078 of AFAD_HUMAN, isoform 5) was amplified by PCR from a cDNA clone (IMAGp998L1313190Q, ImaGenes GmbH, Germany). The PCR product, containing a N-terminal His_6-tag, was cloned into a pET-11a vector (Novagen) and used to transform BL21(DE3) *E. coli* (Novagen) cells for expression. Unlabeled AF6_PDZ was prepared by growing bacteria in LB medium at 37°C to a density of ∼1 OD unit and inducing with 1 mM IPTG for 3 h. Cells were harvested by centrifugation, resuspended in the lysis buffer (20 mM sodium phosphate buffer, 0.5 M NaCl, 50 mM CHAPS, 2% Tween 20, 1 mM dl-dithiothreitol, 10 mM imidazole, 0.5 mM EDTA, pH 7.4, containing one protease inhibitor cocktail tablet (Roche)) and sonicated. After centrifugation, the supernatant was loaded on a Ni^{2+}-Sepharose HisTrap HP column (5 ml, Amersham Biosciences), the column was washed with a 20 mM sodium phosphate buffer containing 0.5 M NaCl, 1 mM dl-dithiothreitol, 10 mM imidazole, pH 7.4 and the protein was eluted with a 10–500 mM imidazole gradient. Fractions containing the pure protein were desalted using a fast-desalting column HiPrep 26/10 (GE Healthcare) and freeze-dried. The uniformly ^{15}N-labeled and ^{13}C,^{15}N-labeled AF6_PDZ samples were prepared by growing *E. coli* cells at 37°C to a density of ∼1 OD unit in M9 minimum medium containing the appropriate isotope source (0.5 mg/ml $^{15}NH_4Cl$; 2.5 mg/ml $^{13}C_6$-glucose). After induction with 1 mM IPTG for 4.5 h, cells were harvested and the protein purified as described above. The identity, purity, and isotopic enrichment of each protein was verified by LC-MS.

Peptide synthesis

The Jagged-1 C-terminal peptides (J1C6: RMEYIV-COOH; J1C6p: RME**pY**IV-COOH; J1C24: Ac-NWTNKQDNRDLESAQSLNRMEYIV-COOH; J1C24pS: Ac-NWTNKQDNRDLESAQ**pS**LNRMEYIV-COOH; J1C24pSpY: Ac-NWTNKQDNRDLESAQ**pS**LNRME**pY**IV-COOH; J1C 24RQ: Ac-NWTNKQDNRDLESAQSLN**Q**MEYIV-COOH; **pY**, phosphotyrosine; **pS**, phosphoserine) were prepared by standard solid-phase Fmoc methods on a NovaSyn TGT (Novabiochem) resin using a home-built automatic synthesizer based on a Gilson Aspec XL SPE. All amino acids were coupled using a four-fold molar excess with respect to the resin load (AA/HCTU/DIPEA = 1/1/2), except phosphorylated amino acids where a double amount of DIPEA was used. After the synthesis, the amino-terminal group was acetylated with 20% Ac_2O and 1.5 equivalents DIPEA for 30 min in DMF. The peptide–resin was cleaved/deprotected in an 8:2.5:3:2:3:1.5:80 (*v*/*v*) mixture of DODT/H_2O/thioanisole/methylethylsulphide/phenol/hydroiodic acid/TFA for 4 h. Crude peptides were purified by semi-preparative RP-HPLC on a Zorbax 300SB-C18 column (9.4 × 250 mm, 5 μm, Agilent) and freeze-dried. The identity of the peptides was checked by LC-MS and the purity (>95%) estimated from RP-HPLC. For SPR experiments, J1C24, J1C24pS, J1C24pSpY, and J1C24RQ were biotinylated through coupling of biotin *p*-nitrophenyl ester to the side chain amino group of the unique lysine in the sequence (K1199), and purified by RP-HPLC.

NMR spectroscopy

All NMR samples were prepared by dissolving the freeze-dried proteins or peptides in phosphate buffer (50 mM Na-phosphate, 50 mM KCl, 1 mM EDTA, 10% *v*/*v* D_2O, pH 5.8). For assignment purposes, the AF6_PDZ protein concentrations were 0.5 mM and 0.8 mM for the ^{13}C,^{15}N-labeled and ^{15}N-labeled samples, respectively. For chemical shift perturbation experiments, aliquots of AF6_PDZ (1 mM) and peptide stock solutions (1–5 mM) were mixed to give different samples with the desired peptide/PDZ ratio and a constant final concentration of 0.1 and 0.2 mM for the ^{13}C,^{15}N-labeled and ^{15}N-labeled AF6_PDZ, respectively. Typically, NMR spectra were recorded at titration points corresponding to peptide/PDZ ratios of 1, 2, 4, 6, 8, and 10. Peptide and protein concentrations were evaluated from absorbance at 280 nm and checked by amino acid analysis.

NMR experiments were carried out at 298 K on Bruker AVANCE 600 and 800 MHz spectrometers equipped with 5-mm triple-resonance probes. NMR data were processed using the

Journal of Molecular Recognition

Azara suite of programs (provided by Wayne Boucher and the Department of Biochemistry, University of Cambridge, UK) or X-WinNMR (Bruker). Spectra were analyzed using the CCPN program ANALYSIS (http://www.ccpn.ac.uk) and CARA (http://www.nmr.ch). Backbone resonance assignments of AF6_PDZ were obtained from TOCSY-HSQC and NOESY-HSQC spectra acquired on the ^{15}N-labeled protein and confirmed by HNCACB and CBCA(CO)NH spectra acquired on the ^{13}C,^{15}N-labeled AF6_PDZ. Assignments of additional methyl groups were obtained from a three-dimensional HCCH-TOCSY spectrum. Chemical shift mapping of the ^{15}N-labeled AF6_PDZ or the ^{13}C,^{15}N-labeled AF6_PDZ titrated with Jagged-1 C-terminal peptides was based on ^{1}H-^{15}N HSQC spectra. Combined chemical shift perturbation (CSP) of backbone amides was calculated according to the formula (Schumann *et al*., 2007):

$$\mathrm{CSP} = \mathrm{sqrt}[(\Delta\delta_H)^2 + \alpha_N(\Delta\delta_N)^2]$$

using a $\Delta\delta_N$ scaling factor (α_N) of 0.102. CSP values were plotted onto the first model of the solution structure of afadin PDZ domain complexed with a LFSTEL peptide (PDB: 2AIN) (Chen *et al*., 2007). Dissociation constants (K_d) were calculated by plotting CSP values against the molar ratios, X (peptide:PDZ), and fitting by nonlinear regression analysis according to the formula (Wintjens *et al*., 2001):

$$\frac{\mathrm{CSP}}{\mathrm{CSP}_{\max}} = 0.5 * \{1 + X + K_d/[P] - [(1 + X + K_d/[P])^2 - 4X]^{1/2}\}$$

where [*P*] is the total concentration of AF6_PDZ.

For selected residues belonging to the GMGL motif, to the βB-strand and to αA- and αB-helices, resonances of methyl groups were tracked using ^{1}H-^{13}C HSQC spectra: combined CH_3 CSP values were calculated according to the formula:

$$\mathrm{CSP} = \mathrm{sqrt}[(\Delta\delta_H)^2 + \alpha_C(\Delta\delta_C)^2]$$

using a $\Delta\delta_C$ scaling factor (α_C) of 0.251 and K_d values calculated as described above.

AF6_PDZ residue numbers are as in PDB: 2AIN.

Surface plasmon resonance

Interactions of AF6_PDZ with selected peptides were assessed using a Biacore T100 apparatus (Biacore, General Electrics Healthcare). Preliminary experiments were carried out by immobilizing AF6_PDZ on a CM5 sensor chip and injecting the different peptides. Dissociation constants calculated using this method were, however, higher than expected and not very reproducible, probably due to the limited solubility of some of the peptides. This problem was overcome using the reciprocal immobilization strategy. When possible, the peptides were biotinylated and immobilized on the streptavidin-coated sensor chip (SA sensor chip) through non-covalent interactions. This approach gave better results, but suffered from a significant degree of non-specific binding to the control flow cell without the peptide, possibly because of charge–charge interactions between streptavidin (calculated pI = 6.1) and AF6_PDZ (calculated pI = 9.4). The following protocol, employing avidin (calculated pI = 9.7) instead of streptavidin, gave the best results. The CM5 sensor chip was primed with 1× HBS-EP running buffer freshly diluted from a 10× stock solution (0.1 M Hepes, 1.5 M NaCl, 30 mM EDTA, 0.5% surfactant P20). ImmunoPure® Avidin from hen egg white (Pierce) was immobilized on the surface of two flow cells through the amine coupling method using 0.05 M *N*-hydroxysuccinimide, 0.2 M *N*-ethyl-*N*′-(3-diethylaminopropyl) carbodiimide and ethanolamine (pH 8.5) (Biacore, General Electrics Healthcare) following the protocols recommended by the producer. The avidin immobilization level was between 2000 and 3000 response units (RU) for all peptides studied. Biotinylated peptides were then injected over the test cell, while the reference cell consisted of only avidin and served to subtract non-specific binding of AF6_PDZ. Final levels of immobilized peptides were 330, 444, 349, and 338 RU for J1C24, J1C24pS, J1C24pSpY, and J1C24RQ, respectively. AF6_PDZ was prepared as a stock solution in 1 × HBS-EP buffer. It was injected across the sensor chip at a flow-rate of 5 μl/min for 1 min and dissociation was monitored for 60 s. The surface was regenerated between injections with a 30 s pulse of 0.5% SDS and stabilized with a flow of running buffer at the same flow-rate for 150 s. All experiments were performed at 25°C. Obtained sensorgrams were evaluated with the Biacore T100 Evaluation Software. Dissociation constants (K_d) were estimated from the binding levels at the end of the injection, which for most injections of AF6_PDZ reached steady-state levels. The K_d values were determined by fitting the following equation to the obtained data:

$$\mathrm{R}_{\mathrm{eq}} = \frac{C * R_{\max}}{(K_d + C)}$$

where R_{eq} is steady-state binding level, *C* is the concentration of AF6_PDZ, and R_{max} is the AF6_PDZ-binding capacity of the surface. The K_ds were determined from three (J1C24, J1C24pS), four (J1C24pSpY), or seven (J1C24RQ) independent titrations.

RESULTS AND DISCUSSION

Jagged-1 C-terminal region binds the βB/αB groove of AF6_PDZ

The mode of interaction of Jagged-1 intracellular region with the PDZ domain of afadin (AF6_PDZ) was investigated by heteronuclear NMR spectroscopy (Figure 1). The binding site on AF6_PDZ was initially mapped by titrating the ^{15}N-labeled AF6_PDZ with J1C6, a short peptide comprising the C-terminal PDZ-binding motif of Jagged-1 (RMEYIV-COOH) and monitoring the chemical shift perturbation (CSP) of the NH peaks from ^{1}H-^{15}N HSQC spectra. The majority of NH peaks are in the fast-exchange regime on the NMR timescale. The NH crosspeak of G18, however, disappeared from the spectrum at low peptide:PDZ ratios but reappeared towards saturation and the M17 amide peak vanished upon step one of the titration and could not be tracked again: these observations suggest an intermediate-exchange timescale for these two amide protons. A plot of CSP versus the amino acid sequence of the PDZ domain (Figure 2) shows that most of the residues displaying significant CSP values are located on one side of the PDZ (βB, βC, αA, αB) whereas the other side (βA, βD, βE, βF) is hardly affected (Figure 3). The peptide-binding site is located between the βB strand and the αB helix, and CSP values are compatible with the canonical binding mode, with the carboxylate of V at P-0 pointing towards the loop between βA and βB and establishing hydrogen bonds with the NH of G18 and L19. The alternating nature of CSP values between L19 and A23 is consistent with the extended conformation of the bound peptide observed in PDZ/peptide complexes and the presence of

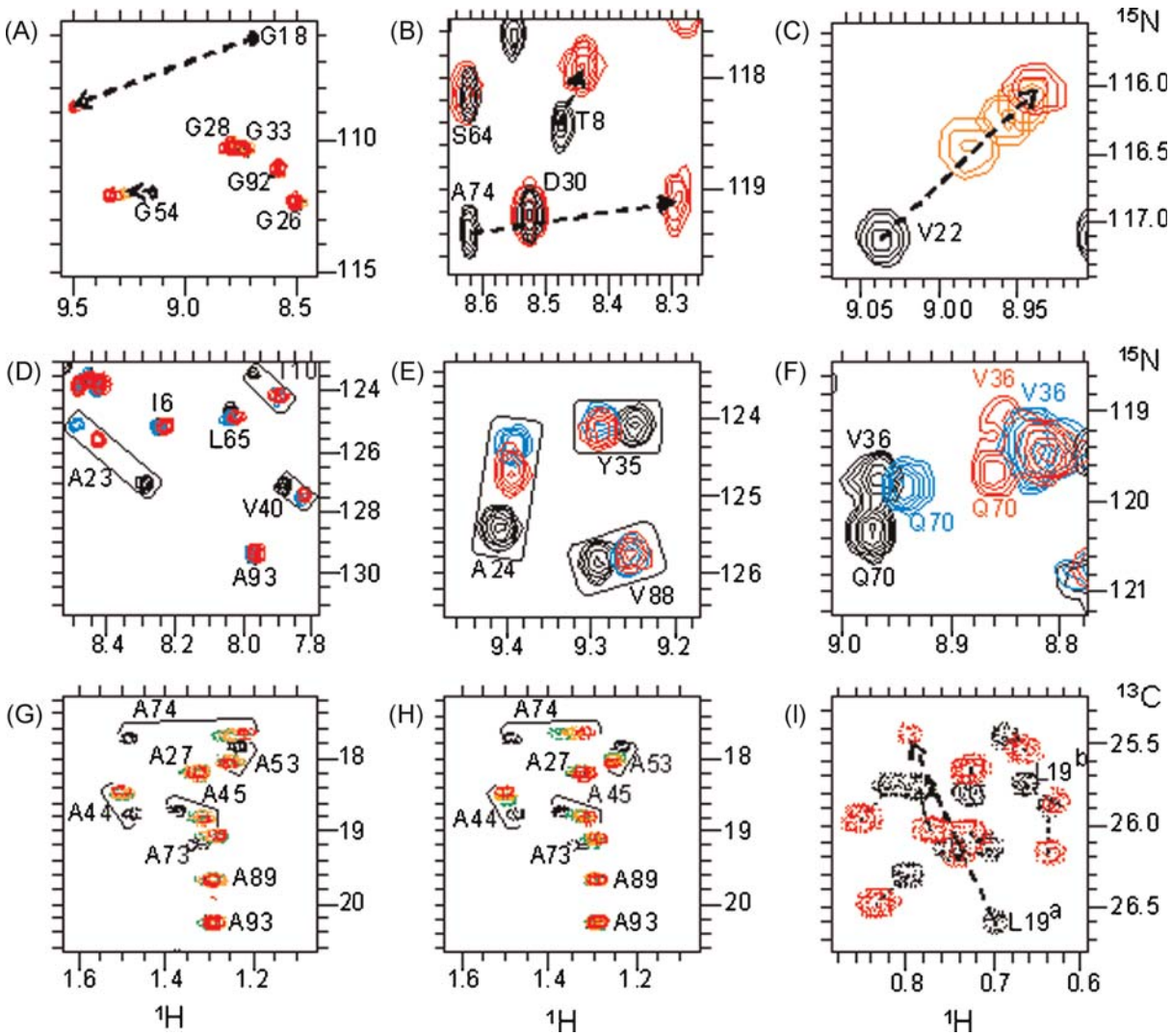

Figure 1. NMR spectroscopy. A, B, and C: backbone NH cross peaks in different regions of the ^{1}H-^{15}N HSQC spectrum of the ^{15}N-labeled AF6_PDZ, free (black) and in the presence of an excess of J1_ic (red). D, E, and F: backbone NH cross peaks in different regions of the ^{1}H-^{15}N HSQC spectrum of the ^{13}C,^{15}N-labeled AF6_PDZ, free (black), and in the presence of an excess of J1C24 (blue) or J1C24pSpY (red). G and H: methyl cross peaks of alanines in the ^{1}H-^{13}C HSQC spectrum of the ^{13}C,^{15}N-labeled AF6_PDZ, free (black), and in the presence of increasing amounts (green, orange, and red) of J1C24 (G) or J1C24pSpY (H). I, methyl crosses peaks in the ^{1}H-^{13}C HSQC spectrum of the ^{13}C,^{15}N-labeled AF6_PDZ, free (black), and in the presence of an excess of J1C24pS (red). Chemical shifts are in ppm.

hydrogen bonds between the backbone of the peptide and the βB strand of the PDZ.

Overall, the CSP pattern observed is very similar to that reported for AF6_PDZ binding to the C-terminal peptide of neurexin (KKNKDKEYYV-COOH), which bears identical residues at P-0, P-2, and P-3 (Zhou *et al.*, 2005). In the neurexin case, it was proposed that the aromatic ring of Y at P-2 makes hydrophobic contacts with A74 in the PDZ, whereas the side chain of E at P-3 forms an ion-pair with the side chain of K37 (Zhou *et al.*, 2005; Chen *et al.*, 2007). Furthermore, significant changes in the chemical shift of Q70 $^{\varepsilon}NH_2$ were observed upon peptide binding (Zhou *et al.*, 2005; Chen *et al.*, 2007). The same residues are also involved in the binding of J1C6 (RMEYIV-COOH), as confirmed by the CSP values measured for A74 and S38 backbone amides, as well as for the $^{\varepsilon}NH_2$ of Q70. Additional residues, notably in the αA helix and in the βC strand, displayed significant CSP values. These residues are not directly involved in peptide binding, and it has been suggested that the perturbation of their chemical shifts might arise from a cascade effect (Lockless and Ranganathan, 1999; Fuentes *et al.*, 2004).

To estimate not only the binding mode but also the affinity, K_d values for selected residues in βB, βC, αA, and αB were calculated from backbone NH CSP values (Table 1) to yield a mean K_d of 17.2 ± 2.3 μM. Because the chemical shift of backbone NHs may be influenced not only by ligand binding but also by subtle changes in secondary structure, hydrogen bonding, and exchange with the solvent, the same titration was performed with the ^{13}C,^{15}N-labeled AF6_PDZ, ^{1}H-^{13}C HSQC spectra were recorded and the chemical shift changes of side chain methyl groups monitored upon peptide binding. Calculation of K_d values for selected residues led to a mean value of 16.4 ± 4.0 μM (Table 2), in excellent agreement with the K_d calculated from backbone NH CSP values (Table 1).

In general, binding to PDZ domains is largely determined by the last four C-terminal residues of the target protein (Wiedemann *et al.*, 2004). In the NMR-derived structure of the

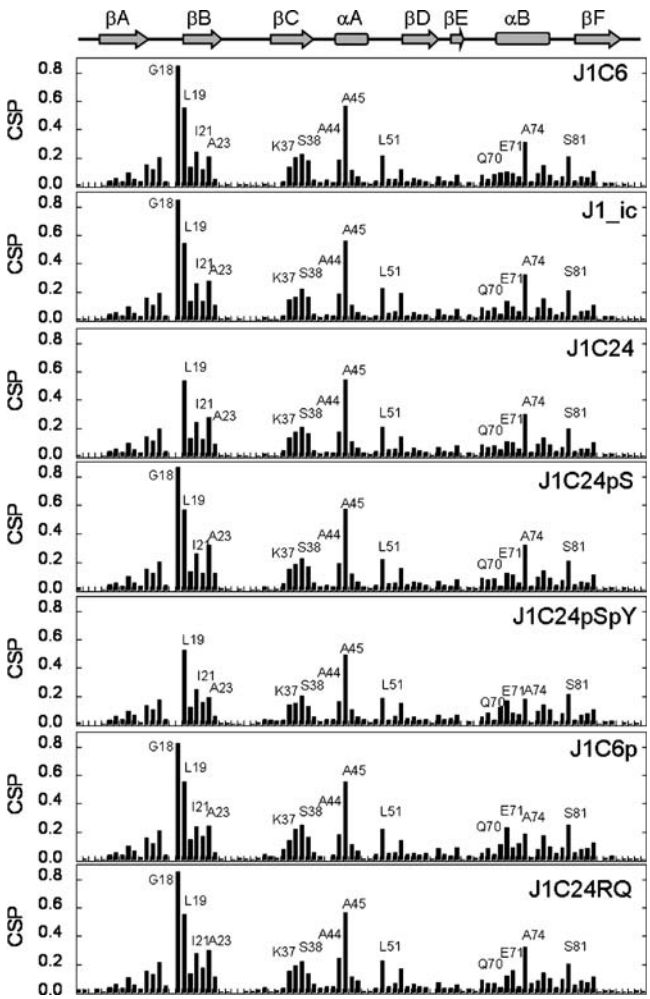

Figure 2. Chemical shift perturbation. Combined chemical shift perturbation (CSP) values of AF6_PDZ backbone amides obtained from titration with different peptides (J1C6, J1C24, J1C24pS, J1C24pSpY, J1C6p, J1C24RQ) and with the recombinant J1_ic; secondary structure elements are shown schematically above.

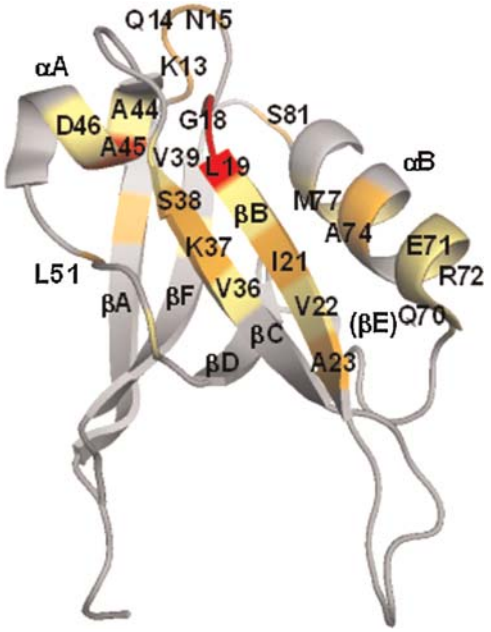

Figure 3. Mapping of the binding site. Cartoon representation of the AF6_PDZ structure (PDB: 2AIN) colored according to backbone amide CSP values (mean < CSP < mean + standard deviation, yellow; mean + standard deviation < CSP < mean + 2×standard deviation, orange; CSP > mean + 2×standard deviation, red) obtained from the titration with the J1C24 peptide.

complex between the afadin PDZ domain and a peptide corresponding to the C-terminus of Bcr, however, several NOEs between the αB helix and the side chain of the residue at P-4 were identified (Zhou *et al*., 2005). Furthermore, deletion studies showed that at least six terminal residues of EphB2 and EphB3 are required to bind the PDZ domain of afadin (Hock *et al*., 1998). Finally, binding of afadin PDZ domain to a combinatorial peptide library suggests that even residues in upstream positions might play an additional role (Wiedemann *et al*., 2004). Thus, the same titration experiments were performed with a longer peptide,

Table 1. Backbone chemical shift mapping. Residue-specific K_d values (μM) calculated from combined CSP values of backbone amides; a mean value and a standard deviation for selected residues are also reported; values with high fitting errors are reported in parentheses and were not included in the calculation of the mean

		J1C6	J1C24	J1C24pS	J1C24pSpY	J1C24RQ	J1_ic
G18		17.1	—	(9.9)	—	—	—
L19	βB	20.1	(15.7)	3.8	—	(1.5)	—
I21	βB	—	7.2	12.6	22.5	—	(40.6)
A23	βB	16.5	9.5	5.9	17.4	(1.0)	—
K37	βC	16.6	6.0	8.3	15.8	(1.6)	21.1
S38	βC	16.1	7.1	8.9	24.0	—	39.1
A45	αA	19.1	(5.2)	10.3	(20.5)	—	(7.7)
L51		15.8	3.2	7.0	18.5	—	13.4
Q70	αB	11.8	12.8	4.6	49.8	—	23.8
A74	αB	19.7	12.2	10.3	19.2	(1.1)	(21.2)
M77	αB	18.1	7.6	12.2	25.0	—	32.3
S81		18.7	14.6	12.1	40.0	—	25.9
Mean		17.2 ± 2.3	8.9 ± 3.7	8.7 ± 3.1	25.8 ± 11.5	—	25.9 ± 8.9

Table 2. Side chain chemical shift mapping. Residue-specific K_d values (μM) calculated from combined CSP values of side chain methyl groups; a mean value and a standard deviation for selected residues are also reported; values with high fitting errors are reported in parentheses and were not included in the calculation of the mean

		J1C6	J1C24	J1C24pS	J1C24pSpY
L19	βB	6.7/19.8	—	16.0	7.2/20.3
I21	βB	16.4/14.5	—	7.4	18.2/45.12
V22	βB	18.4	6.6	7.0	28.4
A23	βB	15.5	10.2	8.7	33.3
A24	βB	11.1	14.2	9.5	60.3
V36	βC	21.8	10.8	16.2	22.4
A44	αA	18.5	10.2	5.4	26.3
A45	αA	15.8	8.0	10.8	36.1
L51		19.6	(62.2)	(47.5)	—
A53		—	8.1	—	25.3
V60	βD	16.0/22.1	9.7/9.7	10.0	32.8/26.3
A73	αB	15.4	12.5	13.8	48.5
A74	αB	14.7	10.0	7.6	32.9
Mean		16.4 ± 4.0	10.0 ± 2.1	10.2 ± 3.6	30.9 ± 13.1

J1C24, corresponding to the last 24 C-terminal residues of Jagged-1, and with the recombinant protein corresponding to the whole cytoplasmic tail of Jagged-1, J1_ic (Popovic *et al.*, 2007). NMR measurements showed no major changes in the backbone NH CSP patterns whether AF6_PDZ was titrated with J1C6, J1C24, or J1_ic (Figure 2). This shows that binding of Jagged-1 cytoplasmic tail to AF6_PDZ is strictly local, involving only the C-terminal residues of Jagged-1 and the binding groove formed by βB and αB in the PDZ. Small differences between J1C6 and J1C24 were detected only for residues A23, A24, and Q70. It is possible that these differences arise from the fact that the positively charged amino terminus in J1C6 is replaced by a neutral amide in the longer J1C24 peptide. An estimation of the K_d from backbone NH CSP of selected residues led to mean values of 17.2 ± 2.3, 8.9 ± 3.7, and 25.9 ± 8.9 μM for J1C6, J1C24, and J1_ic, respectively (Table 1). The higher K_d obtained for J1C6 may arise from unfavorable interactions between the charged amino terminus of the peptide and the PDZ. The difference between J1C24 and J1_ic, on the other hand, might arise from unfavorable electrostatic interactions between AF6_PDZ (calculated pI = 9.4) and J1_ic (calculated pI = 9.3) or from a partially compact form of J1_ic that would limit the availability of the C-terminal region for binding.

Jagged-1 cytoplasmic tail does not fold upon binding

The large majority of structural studies carried out so far on PDZ domains focused on the details of the interaction between the PDZ domain and short peptides. As peptides bind in an extended β-strand conformation that complements the PDZ βB-strand (Remaut and Waksman, 2006), we wondered if binding could trigger a conformational change in the entire cytoplasmic tail of Jagged-1 (Wright and Dyson, 2009). Thus, NMR spectra of the ^{15}N-labeled J1_ic alone and in the presence of the unlabeled AF6_PDZ were recorded. The ^{1}H-^{15}N HSQC spectrum of J1_ic alone does not show any significant ^{1}H chemical shift dispersion in the NH region (Figure 4), as expected for an intrinsically disordered protein (Popovic *et al.*, 2007). No significant chemical shift dispersion was induced by addition of AF6_PDZ, and the chemical shift of the majority of the NH peaks remained unaffected, with the notable exception of a few peaks that can tentatively be assigned to the C-terminal, PDZ-binding region of J1_ic. These results show that, with the conditions used, binding of J1_ic to the PDZ domain of afadin does not trigger folding (Figure 4) and confirm that this interaction is restricted to the

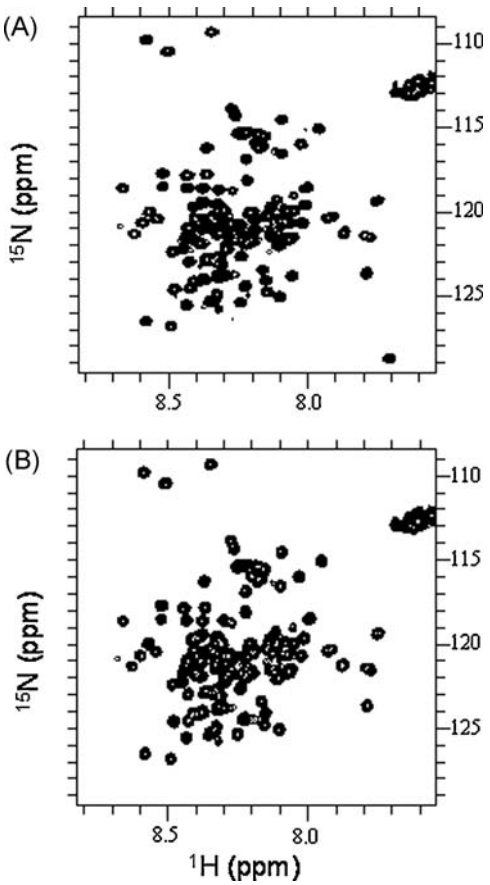

Figure 4. Binding of Jagged-1 cytoplasmic tail to AF6_PDZ. ^{1}H-^{15}N HSQC spectrum of the ^{15}N-labeled J1_ic (A) free and (B) in the presence of unlabeled AF6_PDZ.

Journal of Molecular Recognition

C-terminal residues of Jagged-1 cytoplasmic tail. Whether the PDZ-binding motif is already preorganized in an extended conformation prior to binding (conformational selection) or if it becomes ordered upon binding (induced folding), remains to be determined. Specific environmental factors might also influence this interaction. The intracellular region of Jagged-1 was shown to have a marked propensity to acquire helical structure upon binding to synthetic membranes that mimic the inner leaflet of the cytoplasmic membrane (Popovic *et al*., 2007). The interaction between Jagged-1 cytoplasmic tail and afadin occurs at the interface between the plasma membrane and the cytoplasm, and it is not known if this specific environment can affect binding. Furthermore, afadin is a very large multidomain protein, and it cannot be ruled out that additional regions could act as docking sites for the Jagged-1 cytoplasmic tail.

Tyrosine phosphorylation at P-2 reduces affinity

Whereas the interaction between PDZ domains and short peptides has been studied extensively, relatively little is known about the mechanisms that control this interaction. Post-translational modifications like S/T phosphorylation (Nourry *et al*., 2003) and, more recently, lysine acetylation (Ikenoue *et al*., 2008; Purbey *et al*., 2009) were shown to play a role in the modulation of binding. Serine phosphorylation at P-2 of the Inward Rectifier K^+ channel Kir 2.3 abolished binding to PSD-95 (Cohen *et al*., 1996); serine phosphorylation at an equivalent position of the β2 adrenergic receptor abolished binding to EBP50 (Cao *et al*., 1999); threonine phosphorylation at P-2 of stargazin inhibits binding to PSD-95 (Chetkovich *et al*., 2002); serine phosphorylation of the NR2B subunit of the NMDA receptors disrupts its interaction with PSD-95 and SAP102 (Chung *et al*., 2004); phosphorylation of serine in P-3 has been reported to prevent binding of GluR2 to glutamate receptor interacting protein (Matsuda *et al*., 1999) but not to PICK (Chung *et al*., 2000) and to enhance binding of MRP2-derived peptides to a series of PDZ proteins (Hegedus *et al*., 2003); phosphorylation of serine at P-5 in LDL receptor-related protein 4 suppressed its interaction with PSD-95 and SAP97 (Tian *et al*., 2006); phosphorylation of a tyrosine at P-7 in ErbB2 induces a reorientation of the phenolic ring but does not affect binding to erbin (Birrane *et al*., 2003). The interaction between syntenin-1 and syndecan-1 was recently shown to depend on the dephosphorylation of the tyrosine at P-1 in the EFYA PDZ-binding motif of syndecan-1 (Sulka *et al*., 2009). Binding of afadin PDZ domain to a library of immobilized peptides phosphorylated at different positions showed that strong binding inhibition (<50% binding) is associated with phosphorylation at P-2, a slightly smaller effect at P-1 (~50% binding) and a small but measurable effect at P-8 (~80% binding) (Boisguerin *et al*., 2007). In the C-terminal region of Jagged-1, several residues (T1197, S1207, S1210, Y1216) are potential targets for protein kinases. Although no experimentally confirmed phosphorylation site has been reported to date for Jagged-1, different prediction methods point to T1197, S1210, and Y1216 as potential phosphorylation sites. S1210 matches the [S-X-X-S/T] CK1 phosphorylation pattern and is predicted by GPS (Xue *et al*., 2008) as a potential phosphorylation site also for CAMK. Y1216 matches the [E/D]pY[I/L/V] EGFR pattern and is predicted by GPS as a potential phosphorylation site for several receptor tyrosine kinases. As T1197 is far upstream of the PDZ-binding motif, we focused on S1210 and Y1216, which are at P-8 and P-2, respectively, in the binding motif. To investigate the possible effects of phosphorylation on the binding mode and affinities of J1C24, two phosphorylated variants of the J1C24 peptide were prepared, J1C24pS (Ac NWTNKQDNRDLESAQ **pS**LNRMEYIV-COOH) and J1C24pSpY (Ac NWTNKQDNRDLE SAQ**pS**LNRME**pY**IV-COOH), and their interaction with AF6_PDZ was studied by NMR and SPR.

Titration of ^{15}N-labeled AF6_PDZ with J1C24pS resulted in a CSP profile very similar to that obtained for J1C24 (Figure 2), the only major difference being the reappearance of the resonance corresponding to the G18 amide. Therefore, serine phosphorylation at P-8 does not change significantly the mode of binding to AF6_PDZ. Titration of AF6_PDZ with the doubly phosphorylated J1C24pSpY peptide, on the other hand, showed appreciable differences in the CSP profile for the βB strand (A23, A24) and for the αB helix (Q70, E71, A74). Binding of the short J1C6p peptide to AF6_PDZ resulted in a similar pattern. Thus, tyrosine phosphorylation at P-2 must slightly change the mode of binding. Residue-specific K_d values estimated from CSP of backbone amides (Table 1) show that, whereas no significant difference can be detected between J1C24 (mean $K_d = 8.9 \pm 3.7$ μM) and J1C24pS (mean $K_d = 8.7 \pm 3.1$ μM), tyrosine phosphorylation at P-2 decreases affinity for AF6_PDZ (mean $K_d = 25.8 \pm 11.5$ μM). Also in this case, the K_d values estimated from backbone NH CSP and from side chain methyl groups CSP (10.0 ± 2.1, 10.2 ± 3.6, and 30.9 ± 13.1 μM for J1C24, J1C24pS, and J1C24pSpY, respectively) (Table 2) are in very good agreement and display the same trend.

SPR measurements support the NMR results (Figure 5). The K_d values measured for the J1C24 and J1C24pS (37 ± 3.8 and 28 ± 5.7 μM, respectively) are only slightly different, given the experimental error, whereas tyrosine phosphorylation at P-2 markedly decreases the affinity ($K_d = 150 \pm 69$ μM). Although there is a discrepancy between the K_d values measured by NMR and by SPR, the relative affinities are conserved (J1C24 ~ J1C24pS > J1C24pSpY). The differences between NMR and SPR measurements may arise from the experimental setup specific to each technique, the different conditions used, and from fitting errors in the estimation of K_d values from CSP.

It is likely that the lower affinity of J1C24pSpY for AF6_PDZ is due to the electrostatic repulsion between the negatively charged phosphate moiety and the side chains of E71 and E75, which are on the same side of the αB helix and close to the phosphotyrosine side chain. It can be thus speculated that tyrosine phosphorylation of Jagged-1 at Y1216 may be used *in vivo* to modulate the interaction with afadin, either switching the binding on and off or shifting the binding specificity from one partner to another.

The R1213Q mutation at P-5 increases affinity

A G→A missense mutation leading to the R1213Q substitution in the intracellular region of Jagged-1 was identified as a sporadic mutation in a severe case of extrahepatic biliary atresia, a congenital obstruction of the bile ducts (Kohsaka *et al*., 2002). This mutation involves the residue at P-5 of the PDZ-binding motif. To verify whether this mutation can affect the mode of binding of Jagged-1 to afadin, we titrated the ^{15}N-labeled AF6_PDZ with J1C24RQ (Ac-NWTNKQDNRDLESAQSLN**Q**MEYIV-COOH), recorded ^{1}H-^{15}N HSQC spectra, and mapped the binding site. The CSP plot shows that J1C24RQ binds into the groove between βB and αB, in a similar way as the wild-type J1C24 peptide, but with slightly larger CSP values measured for residues

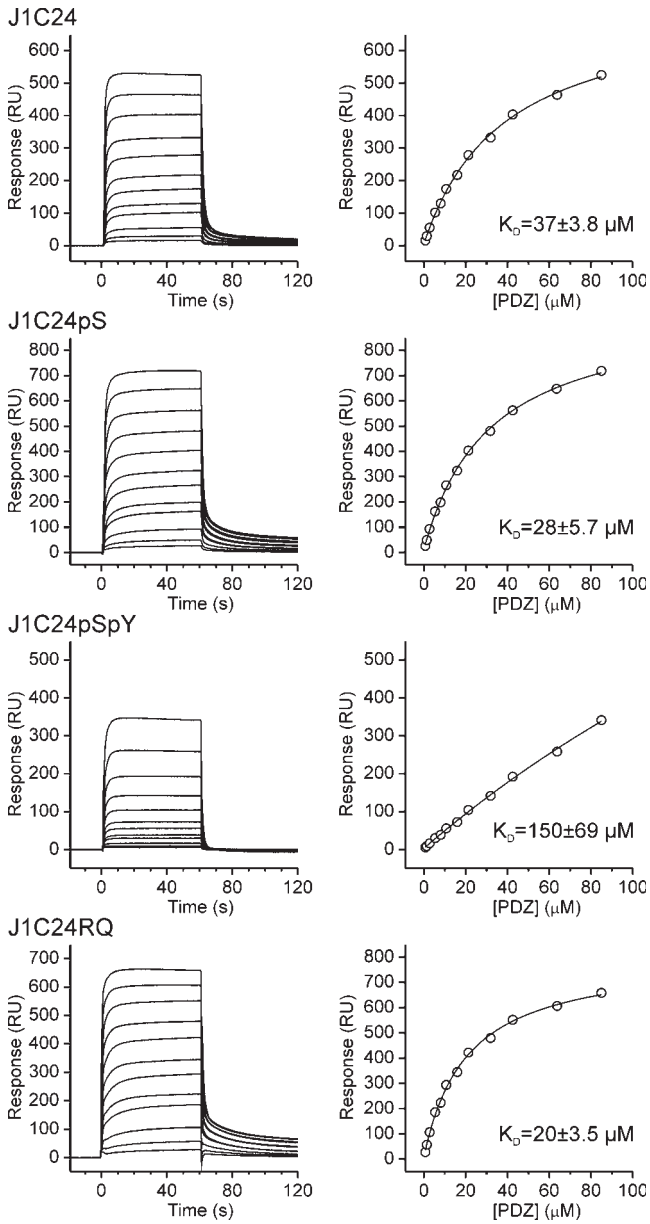

Figure 5. Surface plasmon resonance. Left, sensorgrams of AF6_PDZ (0.66–85 μM, from bottom to top) binding to biotinylated peptides immobilized on the surface of avidin-CM5 sensor chip; right, plots of the response at steady state levels versus the concentration of AF6_PDZ.

V22, A44, and R72 which are located in the βB-strand, the αA-helix and the αB-helix, respectively (Figure 2). Calculation of residue-specific K_d values from CSP of backbone amides was difficult because of the limited solubility of the J1C24RQ peptide under the conditions used for NMR, but they appear to be in the low-micromolar range. Consistently, the K_d measured by SPR for J1C24RQ (20 ± 3.5 μM) was significantly smaller than that of the wild type J1C24 ($K_d = 37 \pm 3.8$ μM). This confirms that residues upstream of the canonical C-terminal tetrapeptide, although not changing the mode of binding to AF6_PDZ, can subtly change the binding affinity. In this specific case a significant but not dramatic change in the binding affinity induced by R1213Q mutation is associated with a severe morphological disorder. This suggests that in developmental processes even a slight imbalance in the PDZ-mediated protein interaction network may have considerable effects. In the only other case we are aware of, a D458V mutation at P-3 of the PDZ-binding motif (ALE**V**TEL-COOH) in SANS (Scaffold protein containing ankyrin repeats and SAM domain) was found to be associated with an atypical form of Usher syndrome (Kalay *et al*., 2005). Because of the frequency of PDZ-mediated protein–protein interactions, it is likely that more disease-associated mutations in the PDZ-binding motifs are yet to be discovered.

CONCLUSIONS

In conclusion, we have systematically investigated the interaction of Jagged-1 cytoplasmic tail with the afadin PDZ domain. We found that this interaction is strictly local, involving only the βB/αB groove in the PDZ and the C-terminal residues of Jagged-1, does not trigger global folding of Jagged-1 cytoplasmic tail, and is potentially modulated by phosphorylation of the tyrosine at position -2 in the PDZ-binding motif; extrahepatic biliary atresia associated with a sporadic R1213Q mutation at position -5 in the PDZ binding motif may be linked to an increase in the affinity for the afadin PDZ.

Acknowledgements

The authors thank Corrado Guarnaccia for continuous technical help, Dusan Uhrin (University of Edinburgh) for helpful discussion on the set up of NMR experiments, Nicola D'Amelio (CBM, Basovizza, Italy) for the acquisition of additional NMR spectra, and EMBO for financial support to M. P. (short-term fellowship).

REFERENCES

Ascano JM, Beverly LJ, Capobianco AJ. 2003. The C-terminal PDZ-ligand of JAGGED1 is essential for cellular transformation. *J. Biol. Chem.* **278**: 8771–8779.

Birrane G, Chung J, Ladias JA. 2003. Novel mode of ligand recognition by the Erbin PDZ domain. *J. Biol. Chem.* **278**: 1399–1402.

Boisguerin P, Ay B, Radziwill G, Fritz RD, Moelling K, Volkmer R. 2007. Characterization of a putative phosphorylation switch: adaptation of SPOT synthesis to analyze PDZ domain regulation mechanisms. *Chem. Biochem.* **8**: 2302–2307.

Brou C. 2009. Intracellular trafficking of Notch receptors and ligands. *Exp. Cell Res.* **315**: 1549–1555.

Cao TT, Deacon HW, Reczek D, Bretscher A, von Zastrow M. 1999. A kinase-regulated PDZ-domain interaction controls endocytic sorting of the beta2-adrenergic receptor. *Nature* **401**: 286–290.

Carmena A, Speicher S, Baylies M. 2006. The PDZ protein Canoe/AF-6 links Ras-MAPK, Notch and Wingless/Wnt signaling pathways by directly interacting with Ras, Notch and Dishevelled. *PLoS One* **1**: e66.

Chen JR, Chang BH, Allen JE, Stiffler MA, MacBeath G. 2008. Predicting PDZ domain-peptide interactions from primary sequences. *Nat. Biotechnol.* **26**: 1041–1045.

Chen Q, Niu X, Xu Y, Wu J, Shi Y. 2007. Solution structure and backbone dynamics of the AF-6 PDZ domain/Bcr peptide complex. *Protein Sci.* **16**: 1053–1062.

Chetkovich DM, Chen L, Stocker TJ, Nicoll RA, Bredt DS. 2002. Phosphorylation of the postsynaptic density-95 (PSD-95)/discs large/zona occlu-

dens-1 binding site of stargazin regulates binding to PSD-95 and synaptic targeting of AMPA receptors. *J. Neurosci.* **22**: 5791–5796.
Chung HJ, Huang YH, Lau LF, Huganir RL. 2004. Regulation of the NMDA receptor complex and trafficking by activity-dependent phosphorylation of the NR2B subunit PDZ ligand. *J. Neurosci.* **24**: 10248–10259.
Chung HJ, Xia J, Scannevin RH, Zhang X, Huganir RL. 2000. Phosphorylation of the AMPA receptor subunit GluR2 differentially regulates its interaction with PDZ domain-containing proteins. *J. Neurosci.* **20**: 7258–7267.
Cohen NA, Brenman JE, Snyder SH, Bredt DS. 1996. Binding of the inward rectifier K+ channel Kir 2.3 to PSD-95 is regulated by protein kinase A phosphorylation. *Neuron* **17**: 759–767.
Fuentes EJ, Der CJ, Lee AL. 2004. Ligand-dependent dynamics and intramolecular signaling in a PDZ domain. *J. Mol. Biol.* **335**: 1105–1115.
Gordon WR, Arnett KL, Blacklow SC. 2008. The molecular logic of Notch signaling–a structural and biochemical perspective. *J. Cell Sci.* **121**: 3109–3119.
Hegedus T, Sessler T, Scott R, Thelin W, Bakos E, Varadi A, Szabo K, Homolya L, Milgram SL, Sarkadi B. 2003. C-terminal phosphorylation of MRP2 modulates its interaction with PDZ proteins. *Biochem. Biophys. Res. Commun.* **302**: 454–461.
Hock B, Bohme B, Karn T, Yamamoto T, Kaibuchi K, Holtrich U, Holland S, Pawson T, Rubsamen-Waigmann H, Strebhardt K. 1998. PDZ-domain-mediated interaction of the Eph-related receptor tyrosine kinase EphB3 and the ras-binding protein AF6 depends on the kinase activity of the receptor. *Proc. Natl Acad. Sci. USA* **95**: 9779–9784.
Ikenoue T, Inoki K, Zhao B, Guan KL. 2008. PTEN acetylation modulates its interaction with PDZ domain. *Cancer Res.* **68**: 6908–6912.
Kalay E, de Brouwer AP, Caylan R, Nabuurs SB, Wollnik B, Karaguzel A, Heister JG, Erdol H, Cremers FP, Cremers CW, Brunner HG, Kremer H. 2005. A novel D458V mutation in the SANS PDZ binding motif causes atypical Usher syndrome. *J. Mol. Med.* **83**: 1025–1032.
Kay BK, Kehoe JW. 2004. PDZ domains and their ligands. *Chem. Biol.* **11**: 423–425.
Kohsaka T, Yuan ZR, Guo SX, Tagawa M, Nakamura A, Nakano M, Kawasasaki H, Inomata Y, Tanaka K, Miyauchi J. 2002. The significance of human jagged 1 mutations detected in severe cases of extrahepatic biliary atresia. *Hepatology* **36**: 904–912.
Kopan R, Ilagan MX. 2009. The canonical Notch signaling pathway: unfolding the activation mechanism. *Cell* **137**: 216–233.
Lockless SW, Ranganathan R. 1999. Evolutionarily conserved pathways of energetic connectivity in protein families. *Science* **286**: 295–299.
Matsuda S, Mikawa S, Hirai H. 1999. Phosphorylation of serine-880 in GluR2 by protein kinase C prevents its C terminus from binding with glutamate receptor-interacting protein. *J. Neurochem.* **73**: 1765–1768.
Nourry C, Grant SG, Borg JP. 2003. PDZ domain proteins: plug and play. *Sci. STKE 2003*: RE7.
Pintar A, De Biasio A, Popovic M, Ivanova N, Pongor S. 2007. The intracellular region of Notch ligands: does the tail make the difference? *Biol. Direct* **2**: 19.
Popovic M, De Biasio A, Pintar A, Pongor S. 2007. The intracellular region of the Notch ligand Jagged-1 gains partial structure upon binding to synthetic membranes. *FEBS J.* **274**: 5325–5336.
Purbey PK, Singh S, Notani D, Kumar PP, Limaye AS, Galande S. 2009. Acetylation-dependent interaction of SATB1 and CtBP1 mediates transcriptional repression by SATB1. *Mol. Cell. Biol.* **29**: 1321–1337.
Remaut H, Waksman G. 2006. Protein-protein interaction through beta-strand addition. *Trends Biochem. Sci.* **31**: 436–444.
Schumann FH, Riepl H, Maurer T, Gronwald W, Neidig KP, Kalbitzer HR. 2007. Combined chemical shift changes and amino acid specific chemical shift mapping of protein-protein interactions. *J. Biomol. NMR* **39**: 275–289.
Songyang Z, Fanning AS, Fu C, Xu J, Marfatia SM, Chishti AH, Crompton A, Chan AC, Anderson JM, Cantley LC. 1997. Recognition of unique carboxyl-terminal motifs by distinct PDZ domains. *Science* **275**: 73–77.
Stiffler MA, Chen JR, Grantcharova VP, Lei Y, Fuchs D, Allen JE, Zaslavskaia LA, MacBeath G. 2007. PDZ domain binding selectivity is optimized across the mouse proteome. *Science* **317**: 364–369.
Sulka B, Lortat-Jacob H, Terreux R, Letourneur F, Rousselle P. 2009. Tyrosine dephosphorylation of the syndecan-1 PDZ binding domain regulates syntenin-1 recruitment. *J. Biol. Chem.* **284**: 10659–10671.
Tian QB, Suzuki T, Yamauchi T, Sakagami H, Yoshimura Y, Miyazawa S, Nakayama K, Saitoh F, Zhang JP, Lu Y, Kondo H, Endo S. 2006. Interaction of LDL receptor-related protein 4 (LRP4) with postsynaptic scaffold proteins via its C-terminal PDZ domain-binding motif, and its regulation by Ca/calmodulin-dependent protein kinase II. *Eur. J. Neurosci.* **23**: 2864–2876.
Tonikian R, Zhang Y, Sazinsky SL, Currell B, Yeh JH, Reva B, Held HA, Appleton BA, Evangelista M, Wu Y, Xin X, Chan AC, Seshagiri S, Lasky LA, Sander C, Boone C, Bader GD, Sidhu SS. 2008. A specificity map for the PDZ domain family. *PLoS Biol.* **6**: e239.
Wiedemann U, Boisguerin P, Leben R, Leitner D, Krause G, Moelling K, Volkmer-Engert R, Oschkinat H. 2004. Quantification of PDZ domain specificity, prediction of ligand affinity and rational design of super-binding peptides. *J. Mol. Biol.* **343**: 703–718.
Wintjens R, Wieruszeski JM, Drobecq H, Rousselot-Pailley P, Buee L, Lippens G, Landrieu I. 2001. 1H NMR study on the binding of Pin1 Trp-Trp domain with phosphothreonine peptides. *J. Biol. Chem.* **276**: 25150–25156.
Wright PE, Dyson HJ. 2009. Linking folding and binding. *Curr. Opin. Struct. Biol.* **19**: 31–38.
Xue Y, Ren J, Gao X, Jin C, Wen L, Yao X. 2008. GPS 2.0, a tool to predict kinase-specific phosphorylation sites in hierarchy. *Mol. Cell. Proteom.* **7**: 1598–1608.
Zhang M, Wang W. 2003. Organization of signaling complexes by PDZ-domain scaffold proteins. *Acc. Chem. Res.* **36**: 530–538.
Zhou H, Xu Y, Yang Y, Huang A, Wu J, Shi Y. 2005. Solution structure of AF-6 PDZ domain and its interaction with the C-terminal peptides from Neurexin and Bcr. *J. Biol. Chem.* **280**: 13841–13847.

